Lysyl oxidase is a strong determinant of tumor cell colonization in bone.

Caroline Reynaud[1,2], Laura Ferreras[1,2], Paola Di Mauro[1,2], Casina Kan[1,2], Martine Croset[1,2], Edith Bonnelye[1,2], Floriane Pez[3], Clémence Thomas[4], Géraldine Aimond[3], Antoine E. Karnoub[4], Marie Brevet[1,5], Philippe Clézardin[1,2].

[1]INSERM, UMR1033, F-69372 Lyon, France

[2] University of Lyon, F-69622 Villeurbanne, France

[3] CNRS, UMR5305, IBCP, F-69367 Lyon, France

[4] Beth Israel Deaconess Medical Center, Harvard Medical School, Boston, MA 02215, USA

[5] Department of Pathology, Groupement Hospitalier Est, Hospices Civils de Lyon, Lyon, France

Short Title: LOX triggers tumor cell colonization in bone

Keywords: metastasis; IL-6; osteoclast; osteoblast.

Disclosure of potential conflict of interests: All authors state that they have no conflicts of interest.

Financial support: CR acknowledges the support of the Ligue Contre le Cancer (Comité du Rhône) and CNRS. PC is supported by INSERM, the University of Lyon, the Grand Prix de la Recherche Ruban Rose, the Fondation de France (grant n°: 00016390), and INCa (grant n°: 2014-164). CK is a recipient of a Marie Curie individual fellowship from the Horizon 2020 European Programme under agreement number n°655777. Additionally,

this work was supported by the LabEX DEVweCAN (ANR-10-LABX-61) of Université de Lyon, within the program "Investissements d'Avenir" (ANR-11-IDEX-0007) operated by the French National Research Agency (ANR).

Corresponding authors:

P. Clézardin, C. Reynaud, INSERM, UMR1033, Faculté de Médecine Lyon-Est (domaine Laennec), Rue Guillaume Paradin, 69372 Lyon cedex 08, France, Tel: 33 4 78 78 57 38; Fax: 33 4 78 77 87 72; emails: philippe.clezardin@inserm.fr; caroline.reynaud@inserm.fr

Abstract

Lysyl oxidase (LOX) is a secreted copper-dependent amine oxidase whose primary function is to drive collagen crosslinking and extracellular matrix stiffness. LOX in colorectal cancer (CRC) synergizes with hypoxia-inducible factor-1 (HIF-1 to promote tumor progression. Here we investigated whether LOX/HIF1 endows CRC cells with full competence for aggressive colonization in bone. We show that a high *LOX* expression in primary tumors from CRC patients was associated with poor clinical outcome, irrespective of *HIF-1*. Additionally, LOX was expressed by tumor cells in the bone marrow from CRC patients with bone metastases. *In vivo* experimental studies show that *LOX* overexpression in CRC cells or systemic delivery of the conditioned medium from *LOX*-overexpressing CRC cells promoted tumor cell dissemination in the bone marrow and enhanced osteolytic lesion formation, irrespective of *HIF-1*. Conversely, silencing or pharmacological inhibition of LOX activity blocked dissemination of CRC cells in the bone marrow and tumor-driven osteolytic lesion formation. *In vitro*, tumor-secreted LOX supported the attachment and survival of CRC cells to and in the bone matrix, and inhibited osteoblast differentiation. *LOX* overexpression in CRC cells also induced a robust production of IL-6. In turn, both LOX and IL-6 were acting in concert to promote RANKL-dependent osteoclast differentiation, thereby creating an imbalance between bone resorption and bone formation. Collectively, our findings show that LOX supports CRC cell dissemination in the bone marrow and they reveal a novel mechanism through which LOX-driven IL-6 production by CRC cells impairs bone homeostasis.

Word count (limit.: 250): 240

Introduction

The lysyl oxidase (LOX) family of secreted copper-dependent amine oxidases consists of five paralogs: LOX and LOX-like 1-4 (LOXL 1-4). The primary function of the LOX family is to catalyse the covalent crosslinking of collagen and elastin in the extracellular matrix, thereby increasing insoluble matrix deposition and tensile strength (1). Increased expression of *LOX* and *LOXL2* has been consistently reported in various cancer types (colorectal, breast, prostate, lung, bladder) (1-5). LOX and LOXL2 are closely associated with desmoplastic areas at the invasive front of infiltrating tumors (1). They mediate collagen/elastin crosslinking that increases extracellular matrix stiffness, a process which is associated with enhanced integrin-mediated mechanotransduction coupled to increased tumor cell invasion in breast and colorectal cancers (1,3,6). LOX- and LOXL2-mediated collagen crosslinking are also responsible for enhancing outgrowth in metastatic xenograft models of breast cancer (5,7). Additionally, LOX enhances the metastatic trait of breast tumor xenografts in animals by stimulating *TWIST1* transcription in tumor cells (8). In the same vein, hypoxia-inducible factor-1 (HIF-1) induces the expression of several members of the LOX family in breast cancer cells, including *LOX* and *LOXL2*, which then catalyses collagen crosslinking in the lungs, facilitating the recruitment of bone marrow-derived cells and the subsequent colonization of the pulmonary tissue by tumor cells (5, 9-11). Furthermore, we have shown that LOX synergizes with HIF-1 in promoting *in vivo* growth of colorectal tumors (2). These experimental results (2, 3, 5-11) probably explain why increased expression of *LOX* and *LOXL2* in primary tumors (colorectal, breast, lung, prostate) is associated with distant relapse and poor survival (1). Indeed, targeting of LOX and LOXL2 with the LOX inhibitor β-aminoproprionitrile (βAPN) or function-blocking antibodies (AB0023, GS341), respectively, is efficacious at reducing metastatic tumor burden in xenograft

models of cancer (7,12,13). Thus, there is a body of experimental evidence indicating that LOX and LOXL2 facilitate the development of metastases in distant organs, such as the lungs, liver, and brain. Surprisingly, little is known regarding the role of LOX proteins during bone metastasis formation.

In bone metastasis, metastatic cancer cells residing in the bone marrow alter the functions of bone-resorbing (osteoclasts) and bone-forming (osteoblasts) cells and hijack signals coming from the bone matrix (14). By disrupting the physiological balance between bone resorption and bone formation, metastatic cells therefore promote skeletal destruction. The detection rate of disseminated tumor cells (DTC) in the bone marrow from colorectal cancer (CRC) patients receiving curatively intended surgery is 27% and their presence is associated with a poor clinical outcome (15,16). This detection rate is relatively high and comparable to what is observed in bone-tropic cancers such as breast cancer (about 30%) (15), which is in intriguing contrast to the low incidence of overt bone metastases in CRC (17). A current hypothesis gaining ground is that DTCs may be representative of dormant tumor cells with the ability to escape dormancy upon receiving appropriate stimuli from the microenvironment (18). Given the role of LOX in driving collagen crosslinking and extracellular matrix stiffness (1), we hypothesized that LOX in CRC may be one of the factors that endow DTCs with full competence for aggressive colonization in bone. Interestingly, it has been very recently shown during the course of this study that hypoxia-induced LOX in breast cancer cells generates premetastatic osteolytic lesions in animals through the stimulation of NFATc1, a master regulator of osteoclastogenesis (19). Here, we investigated the role of LOX and its regulator HIF-1α in CRC bone metastases.

Materials and Methods

Reagents, human CRC cell lines, and animals. All chemicals were obtained from Sigma-Aldrich (Buchs, Switzerland), unless otherwise specified. Primer pairs used for quantitative real-time PCR analysis are listed in Supplementary Table S1. Human CRC cell lines were obtained from the ATCC [Hct116 and HT29 (year 2007); LS174Tr (year 2009)]. They were tested for authentication by DNA fingerprinting using short tandem repeat (STR) method in 2010. The mutation in the *ras* proto-oncogene was tested in 2014. Hct116 cells were maintained in RPMI-1640-Glutamax (Invitrogen) with 10% (v/v) fetal calf serum (FCS) (Life technologies, Carlsbad, CA, USA), 10mM HEPES, 1mM sodium pyruvate, and 0.1mM non essential amino acids (Invitrogen) at 37 °C. HT29 and LS174Tr cells were grown in DMEM-glutamax (Invitrogen), 10% (v/v) FCS and 50µg/ml gentamycin. These cells were first transduced with lentiviral shRNA particles targeting *LOX* (shLOX) or a control sequence (shCTL) then co-transduced with particles containing an empty vector (EV) or a *LOX*-expressing vector (LOX+) under the control of a doxycycline (dox)-inducible promoter, as previously described (2). Transduced cell lines initially called shCTL/EV, shLOX/EV (cells silenced for endogenous *LOX*) and shCTL/LOX+ (cells overexpressing *LOX* in an inducible manner) (2) were named, respectively, Ctrl, LOX- and LOX+ for brevity. Additionally, Ctrl and LOX+ Hct116 cells were co-transduced with lentiviral shRNA particles targeting *HIF-1a* (Ctrl/HIF1α- and LOX+/HIF1α-, respectively), as previously described (2).

Four-week-old female Balb/c immunocompromised mice were purchased from Janvier (Saint-Berthevin, France). Animals were maintained in a 12-h light-dark cycle and given free access to food and water. All procedures involving animals, including their housing and care, the method by which they were culled, and experimental

protocols were conducted in accordance with a code of practice established by the local ethical committee of the University of Lyon.

Immunohistochemistry. CRC tissue specimens (primary tumors and bone metastases) were obtained from the Department of Pathology, Hospices Civils de Lyon. Tumor sections (5µm) were de-paraffinized, treated with pepsin for 15-min at 37°C (Zymed, Invitrogen® Carlsbad USA), and processed for immunohistochemical staining using a LOX antibody (1:250 dilution; ab31238 Abcam).

LOX activity measurement. LOX activity was measured using a fluorescent assay, according to manufacturer's instructions (ab112139 Abcam).

ELISA. Conditionned media from LOX- and LOX+#Hct116 were collected, and IL-6 was measured by ELISA, according to manufacturer's instructions (Clinisciences).

Protein extraction and Western blotting. Proteins were extracted in RIPA buffer, electrophoresed on a SDS-polyacrylamide gel (Life technologies), then transferred onto nitrocellulose membranes (Millipore, Billerica, MA) and proteins were probed with a primary antibody against STAT3 (HP1001671, 1:300 dilution, Sigma), $STAT3^{Y705}$ (9145, 1:1,000 dilution, Cell Signaling), Src (2123, 1:1,000 dilution, Cell Signaling), Src^{Y416} (6943, 1:1,000 dilution, Cell Signaling), FAK (05-537, 1:1,000 dilution, Upstate), FAK^{Y025} (3284, 1:1,000 dilution, Cell Signaling), Akt (9272, 1:1,000 dilution, Cell Signaling), Akt^{T308} (4056, 1:1,000 dilution, Cell Signaling), tubulin (T5168, 1:2,000 dilution, Sigma) or GAPDH (ab9485, 1:2,500 dilution, Abcam). After incubation with primary antibodies, membranes were incubated with horseradish peroxide (HRP)-conjugated secondary goat anti-mouse (1:2,000 dilution, BioRad) or goat anti-rabbit (1:2,500 dilution, BioRad)

antibody. Immunostaining was performed with enhanced chemiluminescence (ECL) detection system (Perkin Elmer).

Functional cell-based assays. Ctrl, LOX- and LOX+ Hct116 cells ($4x10^6$/ml), treated or not treated with 350µM βAPN or 100 µg/ml tocilizumab (Roactemra, Roche), were cultured for 48h in complete RPMI medium without phenol red. Conditioned media were then collected, centrifuged and stored as aliquots at -80°C until used. LOX production was analyzed by western blotting, as previously described (2).

For cell adhesion assays, experiments were conducted as previously described (20). Briefly, 96-well tissue culture plates were coated with increasing concentrations of type-I collagen or fibronectin (0.01mg/cm^2 to 100mg/cm^2) and incubated overnight at 4°C. Cells (4×10^4 cells/0.1 ml/well) were starved for 16 hours then plated to extracellular matrix proteins for 60 min at 37°C in a 5% CO_2 atmosphere. After washing, adherent cells were fixed and stained with 0.1% (w/v) crystal violet. The dye was eluted with 2% (w/v) SDS and the optical density quantified at 595 nm. Alternatively, 96-well tissue culture plates were coated with rat tail type-I collagen (15 µg/cm^2) overnight at 4°C. Following incubation with 1% BSA for 30 min, cells (1×10^5 cells/0.1 ml/well) were incubated for 1h at 37°C in a 5% CO_2 atmosphere. After washing, adherent cells were fixed and stained with hematoxylin and fuschin.

For tumor spheroid-formation assays, $1x10^4$/0.3 ml Hct116 cells (Ctrl, LOX- and LOX+) were seeded in CytoCapture Chambers, Big Hexagonal Cavities (diameter 250µm) (PAA). Cells were grown in suspension in 0.3mL of MammoCult™ basal medium containing 10% (v/v) MammoCult™ proliferation supplement (Stem Cell), 0.0004% (w/v) heparin (Stem Cell), 1µg/mL hydrocortisone, 1mM glutamine, 50U/mL penicillin, 50µg/mL streptomycin (Life Technologies), with or without 350µM β APN. After 5 days

in culture, tumor spheroids were imaged under a microscope (Confocal-Leica SP5 X) and quantified using Fiji software. Spheroids of at least 60µm in diameter were counted.

Osteoclastogenesis assay. Experiments were conducted as described previously (21). Briefly, bone marrow cells from 6-week-old OF1 mice were cultured for 7 days in α-MEM medium (Invitrogen) supplemented with 10% (v/v) FCS, 20 ng/ml M-CSF (R&D Systems) and 200 ng/ml RANKL, alone or in combination (from day 1 to day 7) with the conditioned media from transduced Hct116 cells (Ctrl, LOX+ and LOX-) (25 µg/ml) or with recombinant LOX (150 ng/ml). After 7 days in culture, mature osteoclasts were enumerated under a microscope on the basis of the number of nuclei (more than three nuclei) and TRAP activity.

NFATc1 staining. Cultured osteoclasts on coverslips were fixed for 15 min in 4% PFA then permeabilized with 0.1% Triton X-100 in PBS for 10 min. Saturation was performed with 5% normal goat serum in 0.1% PBS-Tween20 (NGS) for 2h. Monoclonal antibody to NFATc1 (SC-7294, Santa Cruz), diluted 1:100 in NGS, was incubated 1h at room temperature and, after washing, coverslips were further incubated for another 1h with a secondary goat anti-mouse antibody coupled to Alexa Fluor 488 (1:300 dilution in PBS). Coverslips were then mounted in FluorSave Reagent (Calbiochem).

Osteoblastogenesis assay. Experiments were conducted as previously described (22). Briefly, calvaria of 3-day-old OF-1 mice were dissected then cells were enzymatically isolated by sequential digestion with collagenase and plated into 24-well plates. After 24-h incubation, α-MEM medium containing 10% (v/v) FCS was changed and supplemented with 50µg/ml ascorbic acid and with or without conditioned medium from transduced Hct116 cells (Ctrl, LOX+ and LOX-). Medium was changed every other

day for 21 days. 10mM sodium β-glycerophosphate was added for the last week of the experiments. At day 21, bone mineralized nodules were fixed and stained with von Kossa staining.

Animal studies. CRC cell lines ($5x10^5$ cells in 100 µl PBS) were inoculated intra-arterially into anesthetised female Balb/c *nude* mice. When specified, 300 µl of conditioned medium from transduced Hct116 cells were intraperitoneally injected daily into mice. For LOX inhibition, animals were treated with 0.2% (w/v) βAPN, supplied in the drinking water. For blockade of IL-6 receptor, animals were treated every other day with tocilizumab (50 mg/kg, i.p.). The progression of skeletal tumor burden was monitored by whole-body bioluminescence imaging (NightOwl, Berthold Technologies), following subcutaneous administration of luciferin (100 mg/kg in PBS; Promega) 10 min prior to imaging. The progression of osteolytic lesions in the skeleton of anesthetised animals was monitored by radiography, using a cabinet X-ray system (MX-20; Faxitron X-ray Corporation). The area of osteolytic lesions was measured using Explora-Nova Morpho Expert software. Animals were sacrificed on day 7 or 35 after tumor cell inoculation, and hind limbs were collected for histology and histomorphometric analyses.

Bone histology and histomorphometry. Bone histology and histomorphometric analysis of bone tissue sections were performed on decalcified, 5-µm bone-tissue sections stained with Goldner's Trichrome, as previously described (21). For histomorphometric measurements, the bone volume (BV)/tissue volume (TV) and tumor volume (TuV)/soft tissue volume (STV) ratios represent the percentages of bone and tumor tissue, respectively. Additionally, osteoclasts within bone tissue sections

were stained using a TRAP activity kit assay. The resorption surface (Oc.S/BS) was calculated as the ratio of TRAP-positive trabecular bone surface (Oc.S) to the total bone surface (BS) using the image analysis system MorphoExpert (Explora-nova).

***Ex vivo* micrometastasis experiments.** Ex-vivo micrometastasis experiments were conducted as previously described (21). Animals were culled on day 7 or day 35 after tumor cell inoculation. Hind limbs were collected and tibiae and femurs were minced then soaked in an enzyme cocktail containing 300U/ml type-I collagenase and 100 U/ml hyaluronidase (StemCell Technologies) in DMEM medium for 2 hours at 37°C. After incubation, bone marrow cell suspensions were seeded in 6-well plates and cultured in complete medium. After 1-day, cultured cells were placed under puromycin selection for 2 weeks, enabling the selective outgrowth of antibiotic-resistant tumor cells. Tumor cell colonies were then fixed, stained with 0.5% (v/v) crystal violet and counted.

Clinical correlation analyses. Gene expression data and clinical annotations were downloaded from The Cancer Genome Atlas for colorectal cancer and previously published datasets downloaded from the Gene Expression Omnibus (GSE16125, GSE33113, GSE41258, GSE17536, GSE31595, GSE12945) (see Supplementary Table S2).

Statistical Analysis. All experimental data are presented as mean values ± SD. Statistical comparisons of values were made using the Mann-Whitney *U*-test. Disease-free survival Kaplan Meier analyses were performed using the log-rank (Mantel-Cox) test. Correlation analyses were performed by the Spearman Rank test and the Pearson correlation. All tests were two-sided, and *P* values less than 0.05 were considered statistically significant.

Results

LOX expression in colorectal cancer is clinically associated with poor prognosis.

As a first step towards evaluating the role of LOX and its regulator HIF-1α in CRC bone metastases, we conducted a meta-analysis in a cohort of CRC patients (n = 552) and found that high *LOX* expression in primary tumors was associated with poor overall survival (p = 0.0109) and poor relapse-free survival (p = 0.02) (Supplementary Figs. S1a and S1b). Additionally, high *LOX* expression was a negative determinant of relapse-free survival, irrespective of *HIF-1α* levels (Supplementary Fig. S1c). Using immunohistochemistry with a anti-LOX antibody, we examined 5 CRC patients with bone metastases, including 3 patients for whom we had pairs of primary tumors and their matching bone metastases. Although all of the matching primary and metastatic tumors expressed LOX, there was a preferrential moderate-to-strong staining for LOX associated with the carcinoma cells in bone metastases for all 5 patients (Fig. 1 and Supplementary Fig. S1d).

Tumor-secreted LOX in colorectal cancer generates osteolytic lesions in animals.

We next investigated the role for LOX and HIF-1α in CRC bone metastasis formation, using human Hct116 cells (Ctrl) previously transduced for HIF-1α silencing (Ctrl/HIF-1α-) and/or *LOX* overexpression (LOX+ ; LOX+/HIF-1α-) (2). Compared to Ctrl and Ctrl/HIF-1α- tumor-bearing animals, bioluminescent LOX+ Hct116 cells were readily detected in the hind limbs of animals at day 31-post injection, irrespective of *HIF-1* expression (Fig. 2a). Additionally, there was a similar effect on osteolytic lesions in LOX+ and LOX+/HIF-1α- tumor-bearing animals and the extent of lytic lesions was 2.5-fold higher than that of animals bearing Ctrl- or Ctrl/HIF-1α– tumors (Fig. 2b).

Hence, these data indicated that tumor-secreted LOX promotes osteolytic lesion formation *in vivo,* irrespective of *HIF-1α* expression.

To further address the role of LOX in osteolytic lesion formation, we used two additional previously published human CRC cell lines (HT29 and LS174Tr) in which *LOX* expression has been overexpressed or silenced (2). The modulation of *LOX* expression did not affect the expression of other members of the LOX-like family (Supplementary Table S3). We observed that *LOX*-overexpressing Hc116, HT29 and LS174Tr cells caused osteolytic lesions in animals at day 35-post injection (Fig. 2c). The extent of osteolytic lesions in LOX+ tumor-bearing animals was 3- to 5-fold higher than that of animals bearing Ctrl or LOX- tumors (Fig. 2c). Additionally, the treatment of LOX+ Hct116 tumor-bearing animals with the LOX inhibitor βAPN for 35 days, prolonged bone metastasis-free survival to a level similar to that observed with animals bearing LOX- or Ctrl-Hc116 tumors (Supplementary Fig. S2). Histomorphometric analysis of hind limbs with metastases from animals bearing Hct116 tumors showed that the BV/TV ratio (a measure of the bone volume) was decreased in LOX+ tumor-bearing animals, compared with LOX- and Ctrl tumor-bearing animals (Fig. 2d and Table 1). This difference was accompanied with a substantial increase in the TRAP staining of bone tissue sections of metastatic legs from LOX+ tumor-bearing animals (indicating a stimulation of active-osteoclast resorption surfaces) (Fig. 2d and Table 1). Additionally, there was a dramatic increase in the TuV/STV ratio (a measure of the skeletal tumor burden) in LOX+ tumor-bearing animals, compared with animals bearing Ctrl- and LOX- tumors (Fig. 2d and Table 1).

To further examine LOX-dependency, *nude* mice were treated with the conditioned medium from LOX+ or LOX- Hct116 cells beginning 1 day (D-1) before intra-arterial inoculation of parental Hct116 cells (D0). The daily treatment with the conditioned

medium then continued until day 35 (D35), at which time anesthetised animals were analysed by radiography (Fig. 3a). Radiographs of animals showed that mice treated with the LOX+ conditioned medium had a 6-fold increase in the extent of osteolytic lesions, compared to that observed with the LOX- medium (Figure 3b). The bone marrow of 3 metastatic mice per group was then collected and placed in culture under antibiotic selection, enabling the selective outgrowth of antibiotic-resistant tumor cells (Fig. 3c). The average number of colonies recovered from the bone marrow of mice treated with the LOX+ conditioned medium was 2.5-fold higher than that recovered from animals treated with the LOX- conditioned medium (344 ± 60 *vs* 121 ± 25 colonies/well) (P = 0.08) (Fig. 3c). Hence, LOX plays a prominent role in supporting osteolytic lesion formation *in vivo* and tumor cell dissemination *ex vivo*.

LOX disrupts the balance between bone resorption and bone formation.

By disrupting the physiological balance between bone resorption and bone formation, tumor cells promote skeletal destruction (14). To directly test whether *LOX* expression in Hct116 cells could influence osteoclast differentiation, we treated primary mouse bone marrow cell cultures with RANKL and M-CSF together with the conditioned medium from Ctrl, LOX- and LOX+ cancerous cells. Consistent with *in vivo* data (Fig. 2d), the conditioned medium from LOX+ Hct116 cells stimulated the formation of TRAP-positive multinucleated osteoclasts, compared to conditioned media from Ctrl- and LOX- Hct116 cells (Fig. 4a). As aforementioned, βAPN treatment of LOX+ tumor-bearing animals inhibited osteolysis (Supplementary Fig. S2). Similarly, βAPN almost completely inhibited LOX enzymatic activity in the conditioned medium from LOX+ Hct116 cells, compared to that observed with the conditioned medium from LOX- Hct116 cells (Supplementary Fig. S3). Additionally, βAPN blocked the stimulatory effect of LOX+ on

osteoclastogenesis (Fig. 4a), indicating that the promoting effect of LOX on RANKL-dependent osteoclastogenesis critically depends on its enzymatic activity.

LOX overexpression induced a robust production of IL-6 by Hct116 cells, whose production was almost totally inhibited by βAPN treatment (Fig. 4b). Tumor-derived IL-6 can act as an autocrine agent and activate the signal transducer and activator of transcription 3 (STAT3) signalling pathway in CRC cells (23,24). In agreement with these findings (23, 24), STAT3 phosphorylation levels were substantially increased in LOX+Hct116 cells, compared to Ctrl- and LOX- Hct116 cells (Fig. 4c). Additionally, blockade of the IL-6 receptor by tocilizumab abrogated STAT3 phosphorylation in LOX+Hct116 cells, compared with untreated cells (Fig. 4c). Thus, our data revealed a previously unreported functional link between LOX and IL-6, in which LOX-driven IL-6 production by CRC cells promotes IL-6R/STAT3 signaling pathway. This link extended to the clinic, because *LOX* and *IL-6* significantly correlated across 7 publically available databases on CRC, when analysed independently or in combination (Fig. 4d and Supplementary Fig. S4). The addition of IL-6 to the conditioned medium of LOX- Hct116 cells stimulated osteoclast formation to an extent similar to that observed with the conditioned medium from LOX+ Hct116 cells (Fig. 4e). Moreover, tocilizumab inhibited osteoclastogenesis induced by the LOX+ conditioned medium, and an additive inhibitory effect on osteoclast formation was observed when combining tocilizumab and βAPN (Fig. 4f). These results (Fig. 4e-f) suggested that both IL-6 and LOX were effective stimulators of RANKL-dependent osteoclastogenesis. Indeed, in agreement with previous findings (25), we observed that recombinant LOX in combination with RANKL+M-CSF stimulated the formation of osteoclasts *in vitro*, compared to control (RANKL+M-CSF) (Fig. 5a). Additionally, LOX promoted a greater nuclear localization of NFATc1, the master regulator of osteoclastogenesis, than RANKL+MCSF alone (85 *vs*

30% of positive nuclear staining; $P < 0.01$) (Fig. 5b). LOX alone did not stimulate osteoclastogenesis (data not shown). Hence, tumor-secreted LOX and IL-6 were acting in concert to promote the generation of differentiated osteoclasts induced by RANKL.

To determine whether *LOX* expression in Hct116 cells could also influence osteoblast differentiation, we treated primary calvarial mouse osteoblasts with the conditioned medium from Ctrl, LOX+ or LOX- Hct116 cells. We found that the conditioned medium from LOX+Hct116 cells partially inhibited the formation of bone nodules and their mineralization, compared to conditioned media from Ctrl and LOX- Hct116 cells (Fig. 5c-d).

Collectively, our findings suggested that tumor-derived LOX induces an imbalance between bone resorption and bone formation, which leads to bone destruction *in vivo*.

LOX primes tumor cells for dissemination to the bone marrow

To determine the role of LOX in the settlement of tumor cells in the bone marrow, animals injected with parental Hct116 cells were treated daily from D-1 to D7 with the conditioned medium from LOX- or LOX+ Hct116 cells, with or without tocilizumab or βAPN treatment. The bone marrow was then collected and placed in culture under antibiotic selection, enabling growth of tumor cells that have disseminated to the bone marrow (Fig. 6a). We recovered colony-forming tumor cells in the bone marrow from 7 out of 10 animals treated with the LOX+ conditioned medium, whereas only 2 out of 8 animals treated with the LOX- conditioned medium had tumor cell colonies in the bone marrow (Fig. 6b). Moreover, the average number of colony-forming tumor cells recovered from the bone marrow of the 7 metastatic mice treated with the LOX+ conditioned medium was 4-fold higher than that recovered from the 2 mice treated with the LOX- conditioned medium (Fig. 6b). The treatment of animals with βAPN completely

blocked the stimulatory effects of LOX on incidence (1 out of 6 animals) and number of colony-forming tumor cells in the bone marrow (Fig. 6b). In sharp contrast, tocilizumab did not inhibit LOX stimulatory effect on tumor cell dissemination (fig. 6b).

Thus, these data indicate that LOX (irrespective of IL-6) is crucially important in the settlement of tumor cells in the bone marrow.

LOX promotes tumor cell adhesion and survival

We have previously reported that *LOX* overexpression in breast cancer cells induces bone metastasis, a phenotype associated with its ability to induce the expression of a major epithelial-to-mesenchymal (EMT)-transcription factor, *TWIST1* (8). Additionally, we have shown that *TWIST1* facilitates breast cancer bone metastasis formation (21). We therefore proceeded to explore whether LOX promoted tumor cell colonization in bone *via* induction of EMT. Hct116 cells expressed detectable levels of genes encoding for EMT-inducing transcription factors, such as *TWIST1* and *SNAI1* (Supplementary Fig. S5). *LOX* expression in Hct116 cells did not modify the morphological appearance of these cells and it did not modify *TWIST1*, *SNAI1* or vimentin (*VIM)* expression (supplementary Fig. S5), indicating that LOX in colon cancer cells does not contribute to bone marrow colonization by promoting an EMT.

Early steps of bone metastasis involve the attachment and survival of DTCs to and in the bone matrix (14), two properties we examined using *in-vitro* assays. Collagens constitute 90% of the total protein content in bone, type-I collagen being the most abundant bone extracellular matrix protein (26). Cell attachment experiments to type-I collagen were therefore performed using Ctrl, LOX- and LOX+Hct116 cells. As shown in Fig. 6c, there was a significant gain in the attachment of LOX+Hct116 cells to collagen, compared to Ctrl Hct116 cells. The attachment of LOX-deficient tumor cells was lower

than that observed with Ctrl Hct116 cells (Fig. 6c). In contrast, the extent of attachment of Hct116 tumor cell lines to fibronectin was the same, irrespective of *LOX* expression levels (Supplementary Figure S6). Using Hct116 cells silenced for *LOX* expression (LOX-) as a control to measure baseline cell attachment to collagen, we conducted cell attachment experiments with *LOX*+Hct116 cells, in the presence or absence of βAPN or tocilizumab. As shown in Fig. 6c, βAPN abrogated the gain of attachment of *LOX*+Hct116 cells to collagen (LOX+ βAPN), compared to that observed with untreated cells (LOX+) or *LOX+*Hct116 cells treated with tocilizumab. LOX stimulated Akt, Src, and FAK phosphorylation in tumor cells previously attached to collagen (Fig. 6c). Additionally, βAPN (but not tocilizumab) inhibited stimulatory effect of LOX on Akt, Src, and FAK phosphorylation (Fig. 6c). Hence, these observations suggested that LOX activity is important to mediate CRC cell attachment to type-I collagen.

Once tumor cells seed in the bone marrow, they need to survive in this microenvironment. A relevant *in vitro* feature of CRC cell survival is their ability to grow as colonospheres (27). We thus asked whether Ctrl, LOX-, and LOX+ Hct116 cells could form colonospheres in serum-free medium. Indeed, LOX+Hct116 cells formed a higher number of colonospheres than the two other Hct116 cell lines, and growth of LOX+Hct116 cells as colonospheres was significantly inhibited in the presence of βAPN (Supplementary Fig. 7 and data not shown). Thus, LOX can provide CRC cells with a survival advantage in the bone marrow.

Discussion

A large body of preclinical and clinical evidence has shown that *LOX* expression in tumors facilitates the progression of several cancers and the development of metastases

to distant organs, such as the lungs, liver, and brain (1,2,4,7,9,10). Indeed, LOX has been identified as an important regulator of hypoxia-induced tumor progression *via* a HIF-1α-dependent mechanism in numerous cancer types (1,9-11). Surprisingly, aside from a very recent report that hypoxia-induced LOX promotes bone metastasis of breast cancer (19), there was no evidence as to whether this is a generalised function; *i.e*. if tumor-derived LOX participates in the development of bone metastasis in other cancer models, such as colon cancer. We have previously shown that LOX synergizes with HIF-1α in promoting *in vivo* growth of colorectal cancers (2). In the present study, we found that LOX was expressed by tumor cells in the bone marrow from CRC patients with bone metastases and that, irrespective of *HIF-1α* expression, tumor-secreted LOX promoted settlement of CRC cells in the bone marrow and induced a robust expression of IL-6 by these tumor cells. In turn, both LOX and IL-6 played a prominent role in enhancing RANKL-dependent differentiation of mature osteoclasts. In breast cancer, it has been shown that LOX stimulates the generation of differentiated osteoclasts through the activation of NFATc1 (19). LOX secreted from CRC cells also promoted the nuclear translocation of NFATc1 in osteoclasts. Additionally, LOX inhibited osteoblast differentiation, thereby creating an imbalance between bone resorption and bone formation. Based on these findings we propose a model in which LOX supports CRC cell dissemination in the bone marrow and LOX-driven IL-6 production by CRC cells impairs bone homeostasis, thereby promoting osteolytic lesion formation *in vivo* (Fig. 6d).

Having shown that tumor-secreted LOX drives osteolytic lesion formation *in vivo,* we then attempted to determine the specific steps of bone colonization to which LOX functions are manifested. It has been previously reported that LOX enhances the metastatic trait of breast tumors in animals by stimulating *TWIST1* expression in tumor cells (8). Additionally, LOX overexpression in breast cancer has been associated with

EMT of tumor cells (28). Here, *LOX* overexpression in Hct116 cells did not modify the morphological appearance of these cells and it did not modify the expression of transcription factors *TWIST1* and *SNAI1*, indicating that LOX in CRC cells did not contribute to tumor cell dissemination in bone by promoting an EMT. Instead, our results established that LOX (irrespective of IL-6) is crucially important in the settlement of CRC cells in the bone marrow *in vivo*. Specifically, we showed that LOX directly plays a stimulatory role in the survival of CRC cells in the bone marrow by enhancing their attachment to collagen. This contention was supported by the fact that (*i*) LOX activated the phosphorylation of Akt, FAK and Src in CRC cells thta were attached to collagen and (*ii*) the blockade of LOX activity with βAPN inhibited both CRC cell attachment to collagen and Akt, FAK and Src phosphorylation. Here, cell attachment experiments to solid-phase adsorbed collagen were conducted over 1 hour, at which time collagen fibers are still disorganized (13). Thus, irrespective of its ability to crosslink collagen fibers (1), LOX specifically stimulated phosphorylation of Akt, Src, and FAK in CRC cells attached to collagen. How LOX activity activates Akt, Src, and FAK remains unclear. It has been shown that LOX enhances integrin-associated signaling pathways such as FAK and Src (1,4,6). Additionally, integrins mediate CRC survival through Akt (29) and we have previously reported that LOX activates Akt in CRC cells (2). Therefore, it is conceivable that some integrin-mediated mechanisms are involved in promoting (directly or indirectly) the effect of LOX on CRC cell adhesion to collagen. Our findings do not preclude the possibility that other members of the LOX family could contribute to the dissemination of CRC cells in the bone marrow. However, endogenous mRNA levels of *LOXL1*, *LOXL2*, *LOXL3* and *LOXL4* in Hct116 cells were only barely detectable (2), and *LOX* overexpression in these tumor cells did not modify expression levels of other LOX family members (Supplementary Table S3).

Although overt bone metastasis is rare in colon cancer and frequent in breast cancer, the detection rate of DTCs in the bone marrow from CRC patients is comparable to what is observed in breast cancer (15). It seems therefore that colon cancer DTCs should harbor a mechanism to grow out, but this appears to be somehow blocked in colon cancer patients. Only 5 CRC patients with bone metastases were studied here. However, all of them had LOX-positive tumor cells in the bone marrow. Additionally, LOX overexpression endowed CRC cells with full competence for aggressive colonization in bone *in vivo*. Environments that are rich in type-I collagen may be critical for DTCs, promoting their transition from dormancy to metastatic growth (30). Given the role of LOX in mediating CRC cell attachment to collagen and survival in the bone marrow, it is conceivable that LOX participates to metastatic outgrowth of DTCs.

In conclusion, our findings collectively show that LOX supports CRC cell dissemination in the bone marrow and they reveal a novel mechanism through which LOX-driven IL-6 production by CRC cells impairs bone homeostasis. We believe this is a crucially important observation, which supports targeting LOX for metastasis prevention.

Acknowledgements

We acknowledge Dr Cyril Confavreux (Lyon, France) for providing tocilizumab and Dr. Sabine Riethdorf (Hamburg, Germany) for conducting immunofluorescence experiments on CRC cells. We also thank Dr Klaus Pantel (Hamburg, Germany) and Dr Catherine Panabières (Montpellier, France) for valuable discussion.

References

1 - Barker HE, Cox TR, Erler JT. The rationale for targeting the LOX family in cancer. Nat Rev Cancer 2012;12:540-552.

2 - Pez F, Dayan F, Durivault J, Kaniewski B, Aimond G, Le Provost GS, et al. The HIF-1-inducible lysyl oxidase activates HIF-1 via the Akt pathway in a positive regulation loop and synergizes with HIF-1 in promoting tumor cell growth. Cancer Res 2011;71:1647-1657.

3. – Barker HE, Chang J, Cox TR, Lang G, Bird D, Nicolau M, et al. LOXL2-mediated matrix remodeling in metastasis and mammary gland involution. Cancer Res 2011;71:1561-1572.

4 - Baker AM, Bird D, Lang G, Cox TR, Erler JT. Lysyl oxidase enzymatic function increases stiffness to drive colorectal cancer progression through FAK. Oncogene 2013;32:1863-1868.

5 - Cox TR, Bird D, Baker AM, Barker HE, Ho MW, Lang G, et al. LOX-mediated collagen crosslinking is responsible for fibrosis-enhanced metastasis. Cancer Res 2013;73:1721-1732.

6 – Levental KR, Yu H, Kass L, Lakins JN, Egeblad M, Erler JT, et al. Matrix crosslinking forces tumor progression by enhancing integrin signaling. Cell 2009;139:891-906.

7 - Barry-Hamilton V, Spangler R, Marshall D, McCauley S, Rodriguez HM, Oyasu M, et al. Allosteric inhibition of lysyl oxidase-like-2 impedes the development of a pathologic microenvironment. Nat Med 2010;16:1009-1017.

8 - El-Haibi CP, Bell GW, Zhang J, Collmann AY, Wood D, Scherber CM, et al. Critical role for lysyl oxidase in mesenchymal stem cell-driven breast cancer malignancy. Proc Natl Acad Sci USA 2012;109:17460-17465.

9 - Erler JT, Bennewith KL, Nicolau M, Dornhöfer N, Kong C, Le QT, et al. Lysyl oxidase is essential for hypoxia-induced metastasis. Nature 2006; 440:1222-1226.

10 – Erler JT, Bennewith KL, Cox TR, Lang G, Bird D, Koong A, et al. Hypoxia-induced lysyl oxidase is a critical mediator of bone marrow cell recruitment to form the premetastatic niche. Cancer Cell 2009;15:35-44.

11 – Wong CC, Gilkes DM, Zhang H, Chen J, Wei H, Chaturvedi P, *et al*. Hypoxia-inducible factor 1 is a master regulator of breast cancer metastatic niche formation. Proc Natl Acad Sci USA 2011;108:16369-16374.

12 - Bondareva A, Downey CM, Ayres F, Liu W, Boyd SK, Hallgrimsson B, *et al*. The lysyl oxidase inhibitor b-aminopropionitrile diminishes the metastatic colonization potential of circulating breast cancer cells. PLOS One 2009;4:e5620.

13. Grossman M, Ben-Chetrit N, Zhuraviev A, Afik R, Bassat E, Solomonov I, *et al*. Tumor cell invasion can be blocked by modulators of collagen fibril alignment that control assembly of the extracellular matrix. Cancer Res 2016;76:4249-4258.

14 - Weilbaecher KN, Guise TA, McCauley LK. Cancer to bone: a fatal attraction. Nat Rev Cancer 2011;11:411-424.

15 – Pantel K, Schlimok G, Braun S, Kutter D, Lindemann F, Schaller G, *et al*. Differential expression of proliferation-associated molecules in individual micrometastatic carcinoma cells. J Natl Cancer Inst. 1993;85:1419-1424.

16 - Flatmark K, Borgen E, Nesland JM, Rasmussen H, Johannessen HO, Bukholm I, *et al*. Disseminated tumor cells as a prognostic biomarker in colorectal cancer. Br J Cancer 2011;104:1434-1439.

17 - Qiu M, Hu J, Yang D, Cosgrove DP, Xu R. Pattern of distant metastases in colorectal cancer: a SEER based study. Oncotarget 2015;6:38658-38666.

18 - Sosa MS, Bragado P, Aguirre-Ghiso JA. Mechanisms of disseminated cancer cell dormancy: an awakening field. Nat Rev Cancer. 2014;14:611-22.

19 - Cox TR, Rumney RM, Schoof EM, Perryman L, Høye AM, Agrawal A, et al. The hypoxic cancer secretome induces pre-metastatic bone lesions through lysyl oxidase. Nature 2015;522:106-110.

20 – Noblesse E, Cenizo V, Bouez C, Borel A, Gleyzal C, Peyrol S, *et al*. Lysyl oxidase-like and lysyl oxidase are present in the dermis and epidermis of a skin equivalent and in human skin and are associated to elastic fibers. J Invest Dermatol 2004;122:621–630.

21 – Croset M, Goehrig D, Frackowiak A, Bonnelye E, Ansieau S, Puisieux A, *et al*. *TWIST1* expression in breast cancer cells facilitates bone metastasis formation. J Bone Miner Res 2014;29:1886-1899.

22 – Fradet A, Sorel H, Depalle B, Serre CM, Farlay D, Turtoi A, *et al*. A new murine model of osteoblastic/osteolytic lesions from human androgen-resistant prostate cancer. PLoS ONE 2013;8:e75092.

23 - Hsu CP, Chen YL, Huang CC, Chou CC, Liu CL, Hung CH, *et al*. Anti-interleukin-6 receptor antibody inhibits the progression in human colon carcinoma cells. Eur J Clin Invest 2011;41:277-284.

24 - Lin L, Liu A, Peng Z, Lin HJ, Li PK, Li C, *et al*. STAT3 is necessary for proliferation and survival in colon cancer-initiating cells. Cancer Res 2011;71:7226-7237.

25. Tsukasaki M, Hamada K, Okamoto K, Nagashima K, Terashima A, Komatsu N, et al. LOX Fails to Substitute for RANKL in Osteoclastogenesis. J Bone Miner Res. 2016 Sep 8. doi: 10.1002/jbmr.2990. [Epub ahead of print]

26 - Rossert J, De Crombrugghe B. Type I collagen: Structure, synthesis and regulation. In: Bilezikian JP, Raisz LA, Rodan GA (eds) *Principles of Bone Biology*, 2nd ed., vol. 1. Academic Press, San Diego, CA, USA: 189-210 (2013).

27 - Shaheen S, Ahmed M, Lorenzi F, Nateri AS. Spheroid-Formation (Colonosphere) Assay for in Vitro Assessment and Expansion of Stem Cells in Colon Cancer. Stem Cell Rev. 2016;12:492-499.

28 – Han Y, Lian S, Cui X, Meng K, Györffy B, Jin T et al. Potential options for managing LOX+ ER- breast cancer patients. Oncotarget 2016;7:32893-32901.

29- Bao S, Ouyang G, Bai X, Huang Z, Ma C, Liu M, *et al*. Periostin potently promotes metastatic growth of colon cancer by augmenting cell survival via the Akt/PKB pathway. Cancer Cell. 2004;5:329-339.

30 - Barkan D, El Touny LH, Michalowski AM, Smith JA, Chu I, Davis AS, *et al*. Metastatic growth from dormant cells induced by a col-I-enriched fibrotic environment. Cancer Res. 2010;70:5706-5716.

Figure legends

Figure 1. LOX expression in pairs of human primary colorectal carcinoma and their matching bone metastasis. Immunohistochemistry was performed using 3 pairs of patients' tumor specimens. A strong immunostaining for LOX was observed in neoplastic cells (arrows) and, to a less extent, in the desmoplastic tumor stroma. In bone (*), LOX was observed in osteocytic lacunae. Scale bar: 1-mm.

Figure 2. High LOX expression in colorectal cancer cells promotes osteolytic lesion formation *in vivo*. (**a**) Whole body bioluminescence imaging of animals at day 31 after intra-arterial inoculation of luciferase-expressing Hct116 cells. Ctrl: parental Hct116 cells. LOX+: *LOX*-overexpressing Hct116 cells. Ctrl/HIF-1α-: shRNA-*HIF1α*-expressing Hct116 cells. LOX+/HIF-1α- : *LOX*-overexpressing Hct116 cells silenced for *HIF-1α*. The images shown are examples that best illustrate data obtained for each group. (**b**) Quantification of the area of osteolytic lesions (mm^2) on radiographs on day 31 after tumor cell inoculation. *Inset* : Representative radiographs of hind limbs with osteolytic lesions (arrows). (**c**) *Left-hand panels*: Representative radiographs of hind limbs from mice bearing Hct116, HT29 or LS174Tr colorectal tumors. Ctrl: parental tumor cells; LOX+: *LOX*-overexpressing tumor cells; LOX-: shRNA-*LOX*-expressing tumor cells. *Right-hand panels:* Quantification of the area of osteolytic lesions (mm^2) on radiographs at day 35 after tumor cell inoculation. **(d)** *Upper panels*: Goldner's trichrome staining of tissue sections of tibial metaphysis from tumor-bearing animals. Bone is stained green, whereas bone marrow and tumor cells are stained red. The doted line delimits the extent of tumor burden. *Lower panels*: TRAP-stained metastatic bone tissue sections. Osteoclasts are stained red (arrows). All images were obtained from different mice on day 35 after tumor cell inoculation. The images shown are examples that best illustrate

LOX's effects on bone destruction and tumor burden. Scale bar: 0.1 mm. Data are mean ± SD. *,**,***: $p < 0.05$, 0.01 or 0.001, respectively. NS: not significant.

Figure 3. Systemic delivery of tumor-secreted LOX enhances osteolysis and tumor cell outgrowth in the bone marrow. (**a**) Schematic representation of the experimental protocol. Parental Hc116 cells were inoculated intra-arterially to Balb/c nude mice. Animals received a 5-week daily treatment with the conditioned medium from LOX- or LOX+Hct116 cells, starting one day before tumor cell inoculation. Tumor-bearing mice were analyzed by radiography (RX) at day 35 after tumor cell inoculation, then culled and the bone marrow was collected for tumor cell colony assays. (**b**) Quantification of osteolytic lesions (mm^2) on radiographs. *Inset*: Representative radiographs of hind limbs with osteolytic lesions (arrows) from animals treated with the conditioned medium of LOX- or LOX+ Hc116 cells. **: $p < 0.01$ (**c**) Graphs showing the total number of tumor cell colonies formed in the bone marrow of each mouse treated with the LOX- or LOX+ conditioned medium. Representative images of tumor cell colonies are shown for each group.

Figure 4. LOX-driven IL-6 production by colorectal cancer cells stimulates osteoclastogenesis. (**a**) *In vitro* osteoclast differentiation of murine bone marrow cells treated with M-CSF+RANKL in combination with the conditioned medium from Ctrl-, LOX- or LOX+Hct116 cells. The conditioned medium from LOX+Hct116 cells treated with βAPN was also tested. Mature osteoclasts were quantified as multinucleated (more than 3 nuclei), TRAP-positive cells. (**b**) ELISA measurement of IL-6 in the conditioned medium from Ctrl-, LOX-, LOX+ or LOX+/βAPN Hct116 cells. (**c**) Immunoblot analysis of phosphorylated STAT3 in Ctrl-, LOX-, and LOX+Hc116 cells, treated or not treated with

tocilizumab. Graphs show intensities of phosphorylated STAT3 relative to total STAT3. Tubulin was used as a control for equal loading. **(d)** Correlation analysis of *LOX* and *IL-6* expression intensities from 7 databases on colon cancer (n = 1,146 patients). **(e)** Effect of exogenous IL-6 (10 ng/ml) on osteoclastogenesis induced with M-CSF+RANKL in combination with the conditioned medium of LOX- Hct116 cells, compared with that of LOX+Hct116 cells. **(f)** Effects of the anti-IL6 receptor antibody tocilizumab (100 ng/ml) and of β-APN (350μM) on RANKL-dependent osteoclastogenesis in the presence of the conditioned medium of LOX+Hct116 cells. *,**: $p < 0.05$ or 0.01, respectively.

Figure 5. LOX stimulates osteoclastogenesis and inhibits osteoblastogenesis. (a) Recombinant LOX (rLOX; 150 ng/ml) enhanced RANKL-dependent osteoclast differentiation. **(b)** Conditioned medium from LOX+Hc116 cells promoted the nuclear translocation of NFATc1 in osteoclasts, compared to conditioned medium from parental Hct116 cells (Ctrl). Nuclei are stained blue with DAPI. **(c)** and **(d)** *In vitro* differentiation of primary mouse calvaria cells cultured in osteogenic conditions with conditioned media from Ctrl, LOX- and LOX+Hct116 cells. Bone mineralized nodules (stained black with von Kossa staining) were counted under light microscopy. Data are mean ± SD. *,**: $P < 0.05$ and 0.01, respectively.

Figure 6. Systemic delivery of tumor-secreted LOX promotes the settlement of colorectal cancer cells in the bone marrow. (**a**) Schematic representation of the experimental protocol. Parental Hc116 cells were inoculated intra-arterially to *nude* mice, then animals were treated with conditioned media of LOX- or LOX+Hct116 cells (treated or not treated with βAPN or tocilizumab). (**b**) Graphs showing for each group the average number of tumor cell colonies recovered from the bone marrow. Each bar

corresponds to a single mouse. Data are mean ± SD. **: $P < 0.01$. (**c**) Attachement of Ctrl-, LOX- and LOX+Hct116 cells to increasing concentrations of collagen. *Inset*: effect of βAPN or tocilizumab (Toci) on attachment of LOX+Hct116 cells to collagen. Data are mean ± SD. *,**: $P < 0.05$ and 0.01, respectively. *Right panels*: Immunoblot analysis of phosphorylated Akt, Src and FAK in LOX- and LOX+Hc116 cells, treated or not treated with βAPN or tocilizumab (Toci). Graphs show intensities of phosphorylated Akt, Src and FAK relative to total proteins. Tubulin or GAPDH was used as a control for equal loading. (**d**) Schematic representation of the role of LOX during bone metastasis formation. Tumor-secreted LOX enhanced tumor cell attachment to collagen, activating integrin-associated signaling pathways (Fak, Src, Akt), and inducing IL-6 production. In turn, IL-6 and LOX (through the nuclear translocation of NFATc1) enhanced RANKL-mediated osteoclastogenesis, leading to osteolytic lesion formation.

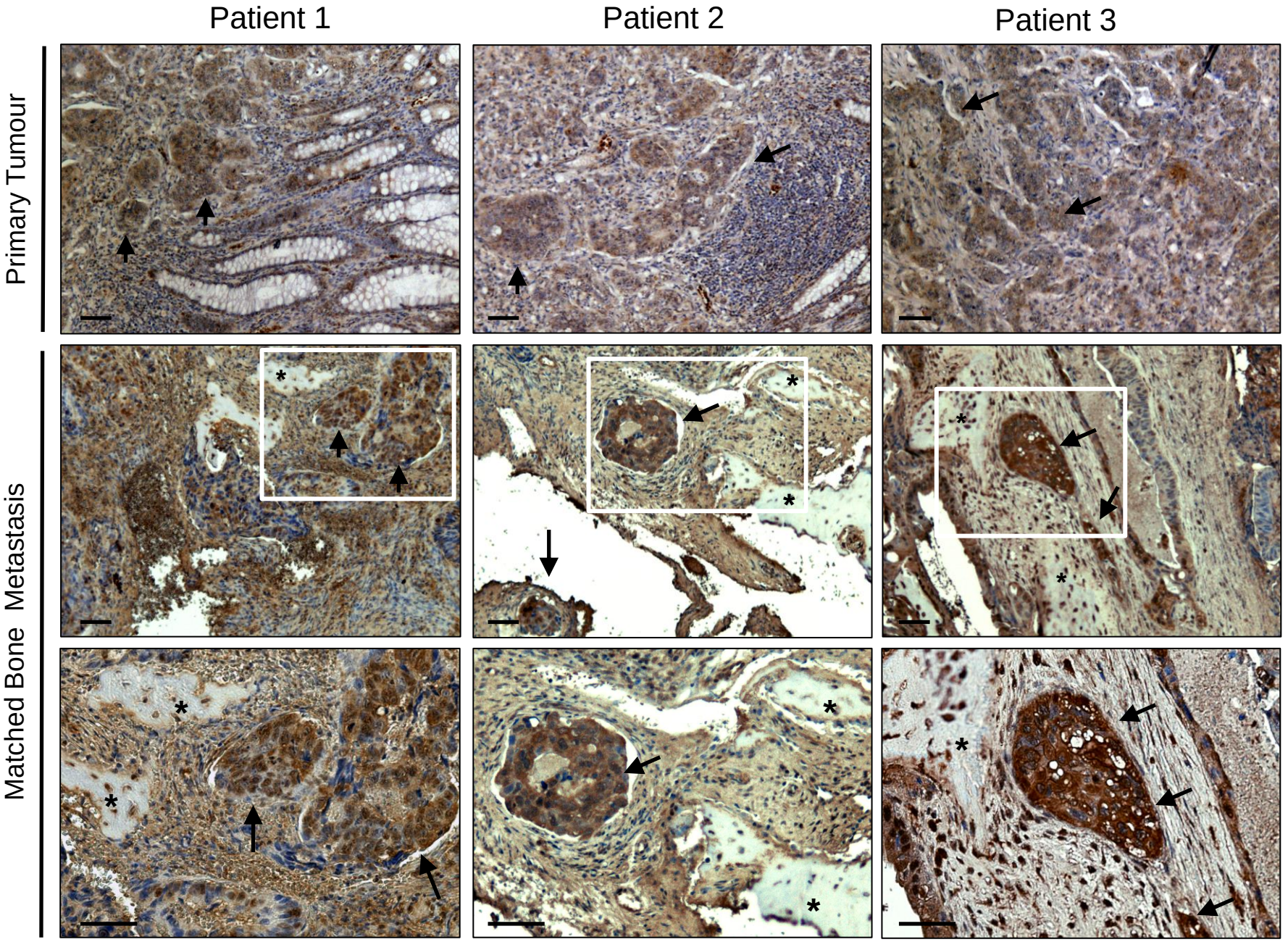

Reynaud et al., Fig. 1

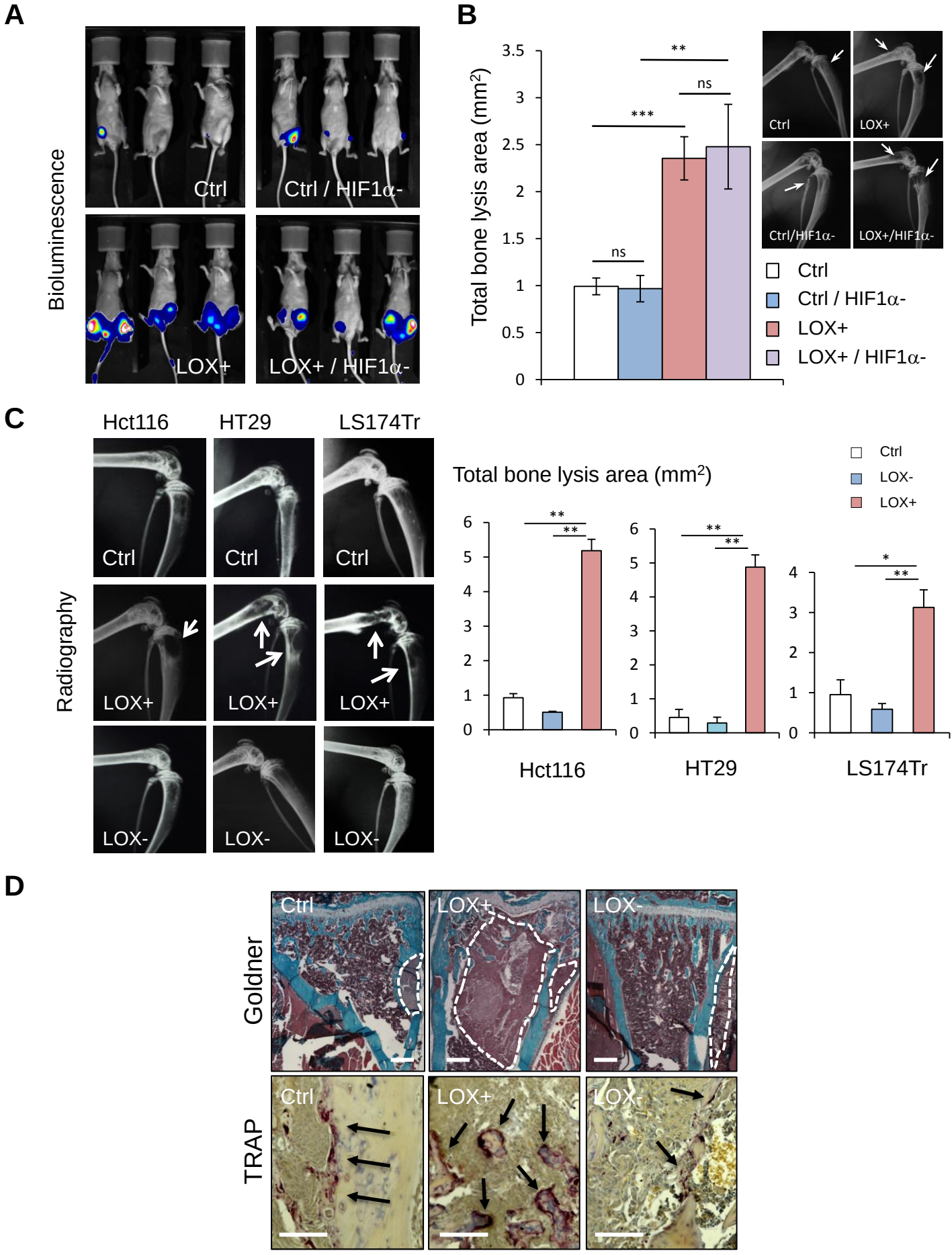

Fig.2: Reynaud et al.

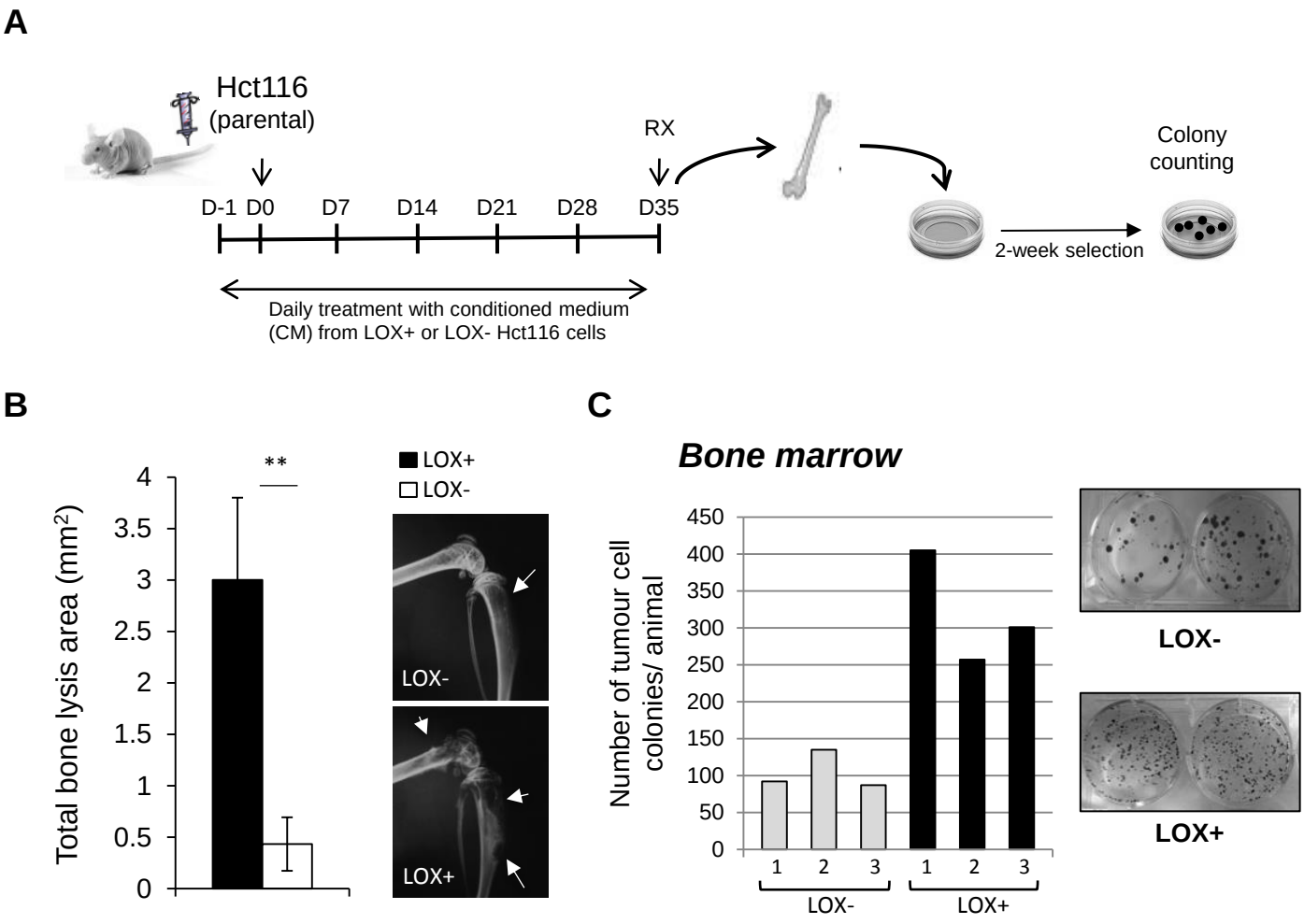

Fig. 3: Reynaud et al.

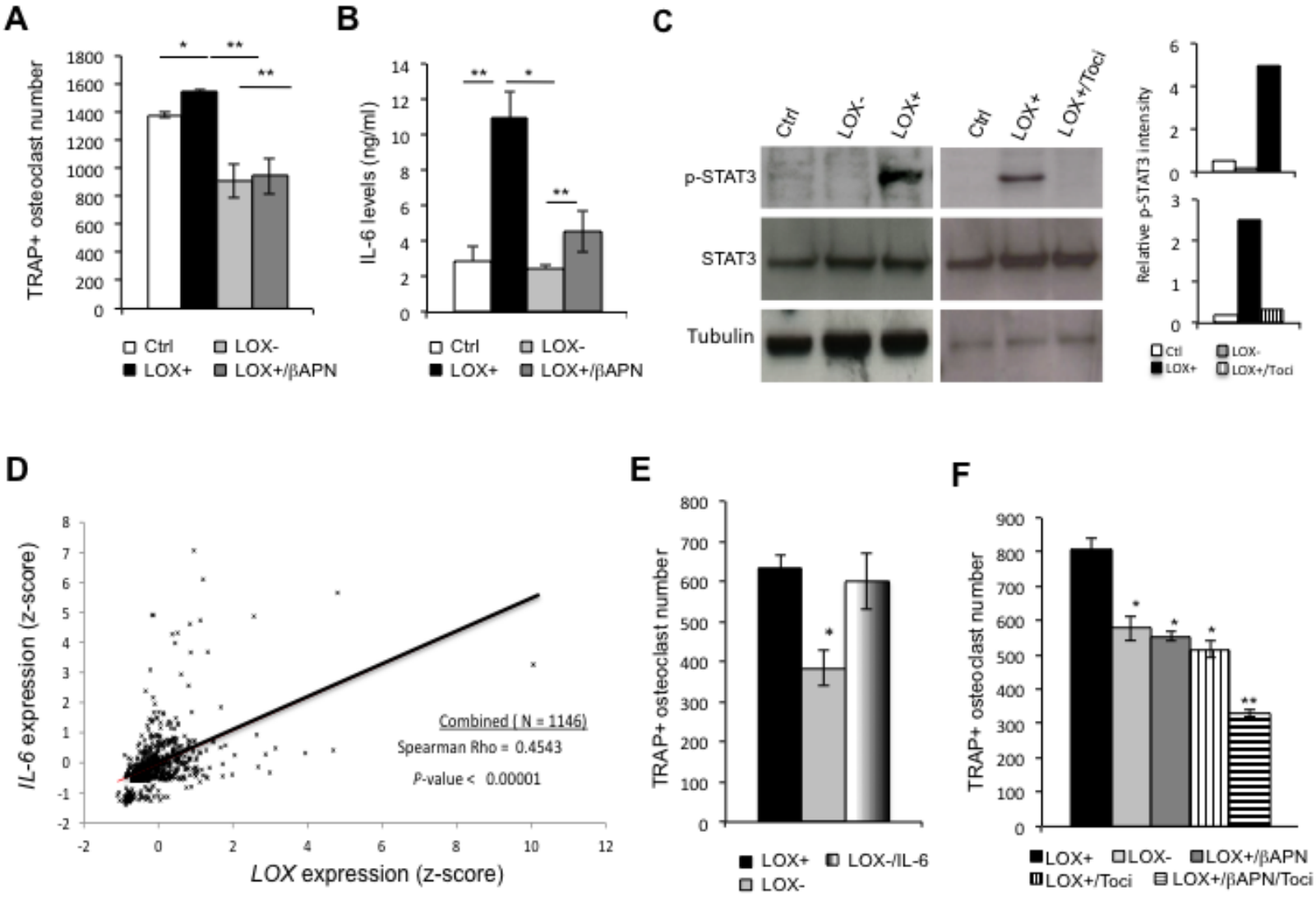

Fig. 4: Reynaud et al.

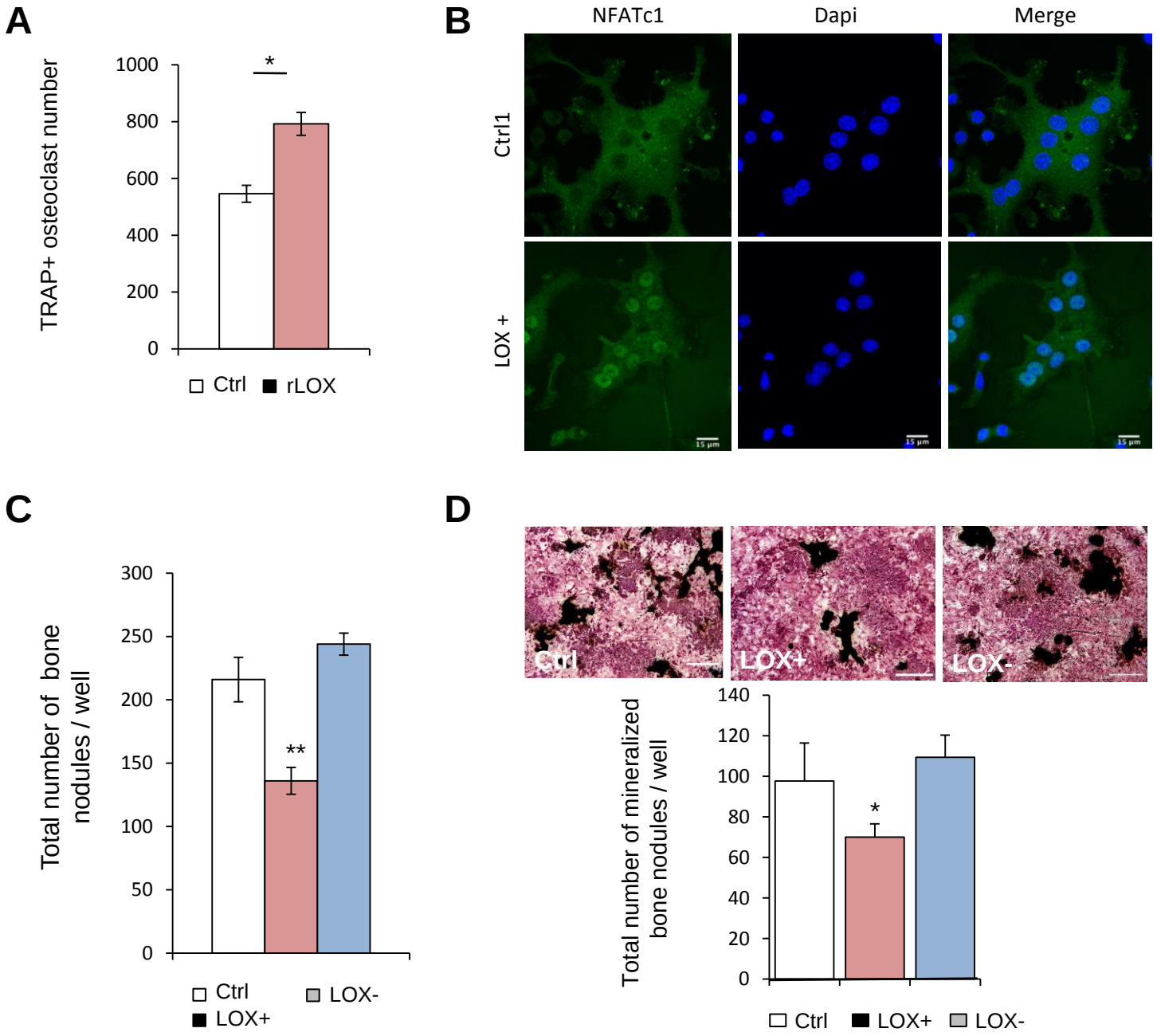

Fig. 5: Reynaud et al.

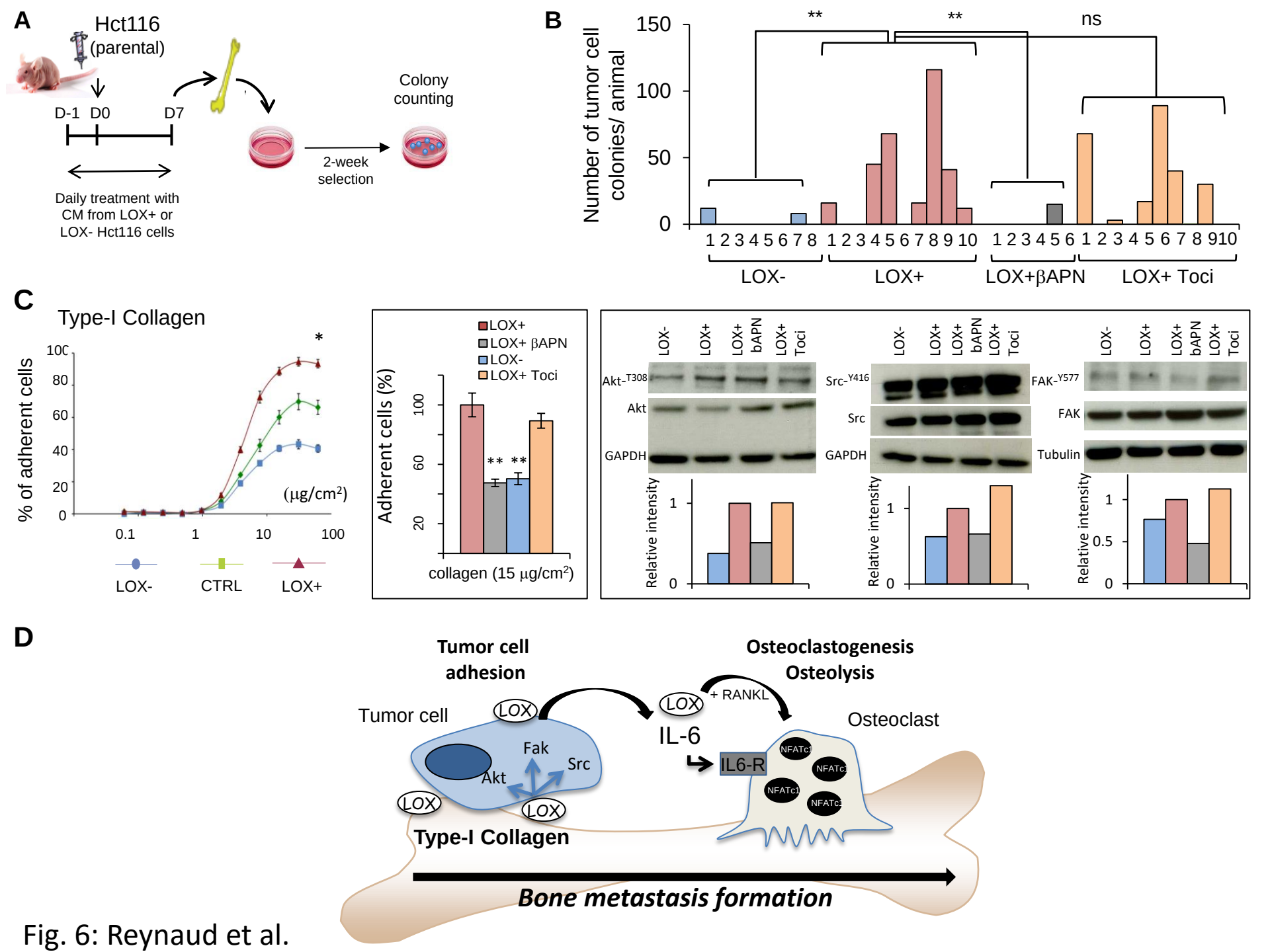

Fig. 6: Reynaud et al.

Table 1. Effects of *LOX* overexpression or silencing in Hct116 colorectal cancer cells on bone metastasis formation in animals.

Cell line	**Histomorphometry**				**TRAP staining**	
	BV/TV (%)	*p*	TuV/STV (%)	*p*	OC.S/BS (%)	*p*
Ctrl	26.5 ± 2.3 (n=8)	-	9.8 ± 6.4 (n=8)	-	31 ± 4.1 (n=5)	-
LOX+	13.9 ± 2.2 (n=8)	*0.0006*	57.6 ± 5.5 (n=8)	*0.0016*	73 ± 6 (n=7)	*0.0017*
LOX-	28.3 ± 2.9 (n=7)	*0.53*	2.6 ± 2.1 (n=7)	*0.33*	19 ± 8.3 (n=3)	*0.09*

Values are mean ± SD. Values of p (two sided) are for pairwise comparison with the control group (Ctrl) using the Mann-Whitney U test.

BV/TV = bone volume-to-tissue volume ratio; TuV/STV = tumour volume-to-total soft tissue volume ratio; OC.S/BS = active osteoclast-resorption surface per trabecular bone surface.; TRAP = tartrate-resistant acid phosphatase.